Approved for public release;
distribution is unlimited.

Distributed Sensor Array Processing of Wideband Acoustic Signals

Richard J. Kozick
Bucknell University
Department of Electrical Engineering
Lewisburg, PA 17837

Brian M. Sadler
Army Research Laboratory
AMSRL-IS-TA
2800 Powder Mill Road
Adelphi, MD 20783

Abstract

We present performance analysis for source localization when wideband aeroacoustic signals are measured at multiple distributed sensor arrays. The acoustic wavefronts are modeled with perfect spatial coherence over individual arrays and with frequency-selective coherence between distinct arrays, thus allowing for random fluctuations due to the propagation medium when the arrays are widely separated. The signals received by the sensors are modeled as wideband Gaussian random processes, and we study the Cramer-Rao bound (CRB) on source localization accuracy for varying levels of signal coherence between the arrays and for processing schemes with different levels of complexity. When the wavefronts at distributed arrays exhibit partial coherence, we show that the source localization accuracy is significantly improved if the coherence is exploited in the source localization processing. Further, we show that a distributed processing scheme involving bearing estimation at the individual arrays and time-delay estimation between pairs of sensors performs nearly as well as the optimum scheme that jointly processes the data from all sensors. We discuss tradeoffs between source localization accuracy and the bandwidth required to communicate data from the individual arrays to a central fusion center.

1 Introduction

Battlefield acoustical surveillance schemes typically deploy multiple microphone arrays over a geographical area in order to measure the sound from a source as it moves through the region. Unless the arrays are spaced very far apart, several arrays will measure the source at any given time. Our objective in this paper is to study the performance of various methods for fusing the data from distributed arrays in order to estimate the source location. In particular, we study source localization performance as a function of the wavefront coherence observed at the distributed arrays, and also with respect to the communication bandwidth required to transmit data from individual arrays to a central fusion processor. Three methods are considered:

1. Each array estimates the source bearing and transmits the bearing estimate to the fusion center. The fusion processor then triangulates the bearings to estimate the source location. This approach does not exploit wavefront coherence between the distributed arrays, but it does minimize the communication bandwidth required to transmit data from the arrays to the fusion center.

2. The raw data from all sensors is jointly processed to estimate the source location. This is the optimum approach and it fully utilizes the coherence between distributed arrays. However, it requires a large communication bandwidth, since the data from all of the sensors must be transmitted to the fusion center.

3. Combination of methods 1 and 2: The objective is to perform some processing at the individual arrays to reduce the communication bandwidth requirement while still exploiting the coherence between distributed arrays. Each array estimates the source bearing and transmits the bearing estimate to the fusion center. In addition, the raw data from *one sensor* in each array is transmitted to the fusion center. The fusion center then estimates the propagation time delay between pairs of distributed arrays, and triangulates these time delay estimates with the bearing estimates to localize the source.

We present results later showing that method 3 performs nearly as well as method 2, as long as the signal-to-noise ratio (SNR) is not too low.

The performance analysis presented in this paper is based on the Cramer-Rao lower bound (CRB) on the accuracy of any unbiased estimator of the source location. We model the signals measured at the distributed sensor arrays as jointly Gaussian wideband random processes. The model is very general, and it accounts for propagation effects between the source and the distributed arrays, including frequency-selective spatial coherence and different signal power levels received at each array. The spatial coherence of the wavefronts is modeled as being perfect over each individual array but variable between distinct arrays. This idealization allows us to study the effect of varying coherence between arrays on source localization accuracy. Physical modeling of frequency-selective coherence is discussed in [13]. The power spectral density of the source is arbitrary, allowing a range of cases to be modeled including narrowband sources and sums of harmonics, as well as wideband sources with continuous power spectra. An interesting observation from the model is that the source location is equivalently parameterized in terms of the bearings from the individual arrays and the time delays between pairs of arrays.[1] This observation motivates our introduction of a decentralized algorithm that first estimates the bearings and time delays, and then localizes the source through a triangulation procedure.

Previous work on source localization with acoustical arrays has focused on angle of arrival estimation with a *single* array [1, 2, 3, 4]. These works use the coherent wideband focusing approach [5, 6] to combine correlation matrices from different narrowband frequency bins into a single correlation matrix that admits subspace processing. The problem of imperfect spatial coherence in the context of narrowband angle-of-arrival estimation with a single array has been studied in [7]-[10]. Pauraj and Kailath [7] presented a MUSIC algorithm that incorporates the nonideal spatial coherence, assuming that the coherence variation is known. Gershman et al. [8] provided a procedure to jointly estimate the spatial coherence loss and the angles of arrival. Song and Ritcey [9] provide maximum-likelihood methods for estimating the parameters of a coherence model and the angles of arrival, and Wilson [10] incorporates physical models for the spatial coherence. The problem of decentralized array processing has been studied in [11] and [12]. Wax and Kailath [11] present subspace algorithms for narrowband signals and distributed arrays, assuming perfect spatial coherence across each array but neglecting the spatial coherence between arrays. Weinstein [12] presents performance analysis for pairwise processing the wideband sensor signals from a single array and shows negligible loss in localization accuracy when the SNR is high.

The paper is organized as follows. Section 2 describes our model for the wideband signals observed by the distributed sensor arrays. Section 3 presents the CRBs on source localization

[1] The parameterization of source location in terms of bearings and time delays is true as long as the array geometry and frequency band of the source satisfy certain uniqueness properties.

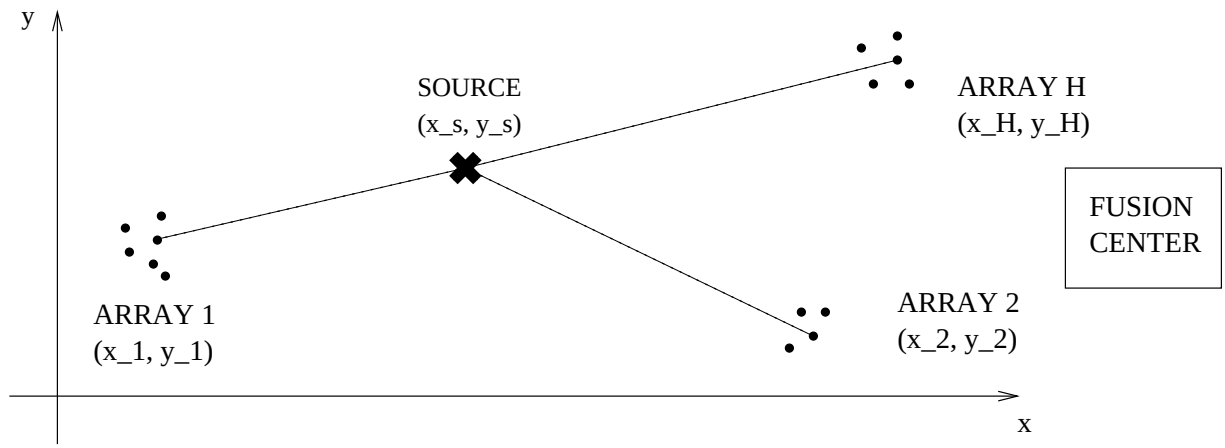

Figure 1: Geometry of source location and H distributed sensor arrays. A communication link is available between each array and the fusion center.

accuracy for processing methods with different communication bandwidth requirements between arrays and the central fusion center. Section 4 contains examples of source localization performance for specific scenarios, and Section 5 contains a brief discussion of our continuing work. A glossary of mathematical symbols is included in the Appendix.

2 Data Model

A model is formulated in this section for the discrete-time signals received by the sensors in distributed arrays. Consider a single source that is located at coordinates (x_s, y_s) in the (x, y) plane. Then H arrays are distributed in the same plane, as illustrated in Figure 1. Each array $h \in \{1, \ldots, H\}$ contains N_h sensors, and has a reference sensor located at coordinates (x_h, y_h). The location of sensor $n \in \{1, \ldots, N_h\}$ is at $(x_h + \Delta x_{hn}, y_h + \Delta y_{hn})$, where $(\Delta x_{hn}, \Delta y_{hn})$ is the relative location with respect to the reference sensor. If c is the speed of propagation, then the propagation time from the source to the reference sensor on array h is

$$\tau_h = \frac{r_h}{c} = \frac{1}{c}\left[(x_s - x_h)^2 + (y_s - y_h)^2\right]^{1/2}. \tag{1}$$

We will assume that the wavefronts are well approximated by plane waves over the aperture of individual arrays. Then the propagation time from the source to sensor n on array h will be expressed by $\tau_h + \tau_{hn}$, where

$$\tau_{hn} \approx -\frac{1}{c}\left[\frac{x_s - x_h}{r_h}\Delta x_{hn} + \frac{y_s - y_h}{r_h}\Delta y_{hn}\right] = -\frac{1}{c}\left[(\cos\phi_h)\Delta x_{hn} + (\sin\phi_h)\Delta y_{hn}\right], \tag{2}$$

where τ_{hn} is the propagation time from the reference sensor on array h to sensor n on array h, and ϕ_h is the bearing of the source with respect to array h. Note that while the far-field approximation (2) is reasonable over individual array apertures, the wavefront curvature that is inherent in (1) must be retained in order to accurately model the (possibly) wide separation between arrays.

The time signal received at sensor n on array h due to the source will be represented as $s_h(t - \tau_h - \tau_{hn})$, where the vector of signals $\mathbf{s}(t) = [s_1(t), \ldots, s_H(t)]^T$ received at the H arrays are modeled as real-valued, continuous-time, zero-mean, wide-sense stationary, Gaussian random processes with

$-\infty < t < \infty$. These processes are fully specified by the $H \times H$ cross-correlation function matrix

$$\mathbf{R}_s(\tau) = E\{\mathbf{s}(t+\tau)\,\mathbf{s}(t)^T\}, \tag{3}$$

where E denotes expectation, superscript T denotes transpose, and we will later use the notation superscript $*$ and superscript H to denote complex conjugate and conjugate transpose, respectively. The (g,h) element in (3) is the cross-correlation function

$$r_{s,gh}(\tau) = E\{s_g(t+\tau)\,s_h(t)\} \tag{4}$$

between the signals received at arrays g and h. The correlation functions (3) and (4) are equivalently characterized by their Fourier transforms, which are the cross-spectral density function

$$G_{s,gh}(\omega) = \mathcal{F}\{r_{s,gh}(\tau)\} = \int_{-\infty}^{\infty} r_{s,gh}(\tau)\exp(-j\omega\tau)\;d\tau \tag{5}$$

and the associated cross-spectral density matrix

$$\mathbf{G}_s(\omega) = \mathcal{F}\{\mathbf{R}_s(\tau)\}. \tag{6}$$

The diagonal elements $G_{s,hh}(\omega)$ of (6) are the power spectral density (PSD) functions of the signals $s_h(t)$, and hence they describe the distribution of average signal power with frequency. The model allows the average signal power to vary from one array to another. Indeed, the PSD may even vary from one array to another to reflect propagation differences, source aspect angle differences, and other effects that lead to coherence degradation in the signals at distributed arrays.

Let us elaborate the definition and the meaning of *coherence* between the signals $s_g(t)$ and $s_h(t)$ received at distinct arrays g and h. In general, the cross-spectral density function (5) can be expressed in the form

$$G_{s,gh}(\omega) = \gamma_{s,gh}(\omega)\;\left[G_{s,gg}(\omega)G_{s,hh}(\omega)\right]^{1/2}, \tag{7}$$

where $\gamma_{s,gh}(\omega)$ is the spectral coherence function, which has the property $0 \le |\gamma_{s,gh}(\omega)| \le 1$. The coherence function $\gamma_{s,gh}(\omega)$ is generally complex-valued, but we will model it as real-valued. This is a reasonable assumption for acoustic propagation environments in which the loss of coherence is due to random changes in the apparent source location, as long as the change in apparent source location is the same at both arrays g and h [10, 13].

Let us consider the cases of fully coherent signals where $\gamma_{s,gh}(\omega) = 1$ at all frequencies, incoherent signals where $\gamma_{s,gh}(\omega) = 0$ at all frequencies, and partial coherence where $0 < |\gamma_{s,gh}(\omega)| < 1$ at some frequencies. If the signals are fully coherent $\gamma_{s,gh}(\omega) = 1$, then the signals are identical up to a positive scale factor, i.e., $s_g(t) = \alpha_{gh}s_h(t)$ with $\alpha_{gh} > 0$. In this case, the coherent cross-spectral density and cross-correlation have the same form as the auto-spectral density and auto-correlation:

$$G_{s,gh}(\omega)^{(\mathrm{COH})} = \left[G_{s,gg}(\omega)G_{s,hh}(\omega)\right]^{1/2} = G_{s,hh}(\omega)\left(\frac{r_{s,gg}(0)}{r_{s,hh}(0)}\right)^{1/2} \tag{8}$$

$$r_{s,gh}(\tau)^{(\mathrm{COH})} = r_{s,hh}(\tau)\left(\frac{r_{s,gg}(0)}{r_{s,hh}(0)}\right)^{1/2}. \tag{9}$$

If the signals are incoherent with $\gamma_{s,gh}(\omega) = 0$, then the cross-correlation $r_{s,gh}(\tau) = 0$ and the Gaussian processes $s_g(t)$ and $s_h(t)$ are statistically independent. If the signals are partially coherent with $0 < |\gamma_{s,gh}(\omega)| < 1$ and we define $p_{s,gh}(\tau) = \mathcal{F}^{-1}\{\gamma_{s,gh}(\omega)\}$ as the inverse Fourier transform

of the coherence function, then we can express the partially coherent cross-spectral density and cross-correlation functions in relation to the coherent counterparts (8) and (9) as

$$G_{s,gh}(\omega) = \gamma_{s,gh}(\omega)\, G_{s,gh}(\omega)^{(\mathrm{COH})} \tag{10}$$

$$r_{s,gh}(\tau) = p_{s,gh}(\tau) * r_{s,gh}(\tau)^{(\mathrm{COH})} = \int_{-\infty}^{\infty} p_{s,gh}(\tau - t) r_{s,gh}(t)^{(\mathrm{COH})}\, dt, \tag{11}$$

where $*$ in (11) denotes convolution. Physical models suggest that the spectral coherence $\gamma_{s,gh}(\omega)$ is a low-pass function [13], so (11) shows that partial coherence produces a "smearing" of the cross-correlation function relative to the perfectly coherent case. This smearing reduces the resolution in estimating the relative time delay of the signals arriving at arrays g and h, which consequently reduces the accuracy of source localization.

Next we model the signal received at sensor n on array h as a sum of the delayed source signal and noise,

$$z_{hn}(t) = s_h(t - \tau_h - \tau_{hn}) + w_{hn}(t), \tag{12}$$

where the noise signals $w_{hn}(t)$ are modeled as real-valued, continuous-time, zero-mean, wide-sense stationary, Gaussian random processes that are uncorrelated at distinct sensors. That is, the noise correlation properties are

$$E\{w_{gm}(t+\tau) w_{hn}(t)\} = r_w(\tau)\, \delta_{gh} \delta_{mn}, \tag{13}$$

where $r_w(\tau)$ is the noise autocorrelation function, and the noise power spectral density is $G_w(\omega) = \mathcal{F}\{r_w(\tau)\}$. We then collect the observations at each array h into $N_h \times 1$ vectors $\mathbf{z}_h(t) = [z_{h1}(t), \ldots, z_{h,N_h}(t)]^T$ for $h = 1, \ldots, H$, and we further collect the observations from the H arrays into a $(N_1 + \cdots + N_H) \times 1$ vector

$$\mathbf{Z}(t) = \begin{bmatrix} \mathbf{z}_1(t) \\ \vdots \\ \mathbf{z}_H(t) \end{bmatrix}. \tag{14}$$

The elements of $\mathbf{Z}(t)$ in (14) are zero-mean, wide-sense stationary, Gaussian random processes. We can express the cross-spectral density matrix of $\mathbf{Z}(t)$ in a convenient form with the following definitions. The array manifold for array h at frequency ω is

$$\mathbf{a}_h(\omega) = \begin{bmatrix} \exp(-j\omega\tau_{h1}) \\ \vdots \\ \exp(-j\omega\tau_{h,N_h}) \end{bmatrix} = \begin{bmatrix} \exp\left[j\frac{\omega}{c}\left((\cos\phi_h)\Delta x_{h1} + (\sin\phi_h)\Delta y_{h1}\right)\right] \\ \vdots \\ \exp\left[j\frac{\omega}{c}\left((\cos\phi_h)\Delta x_{h,N_h} + (\sin\phi_h)\Delta y_{h,N_h}\right)\right] \end{bmatrix}, \tag{15}$$

using τ_{hn} from (2) and assuming that the sensors have omnidirectional response to sources in the plane of interest. Let us define the relative time delay of the signal at arrays g and h as

$$D_{gh} = \tau_g - \tau_h, \tag{16}$$

where τ_h is defined in (1). Then the cross-spectral density matrix of $\mathbf{Z}(t)$ in (14) has the form

$$\mathbf{G}_{\mathbf{Z}}(\omega) = \begin{bmatrix} \mathbf{a}_1(\omega)\mathbf{a}_1(\omega)^H G_{s,11}(\omega) & \cdots & \mathbf{a}_1(\omega)\mathbf{a}_H(\omega)^H \exp(-j\omega D_{1H}) G_{s,1H}(\omega) \\ \vdots & \ddots & \vdots \\ \mathbf{a}_H(\omega)\mathbf{a}_1(\omega)^H \exp(+j\omega D_{1H}) G_{s,1H}(\omega)^* & \cdots & \mathbf{a}_H(\omega)\mathbf{a}_H(\omega)^H G_{s,HH}(\omega) \end{bmatrix} + G_w(\omega)\mathbf{I}. \tag{17}$$

Recall that the source cross-spectral density functions $G_{s,gh}(\omega)$ in (17) can be expressed in terms of the spectral coherence $\gamma_{s,gh}(\omega)$ using (7).

Note that (17) depends on the source location parameters (x_s, y_s) through $\mathbf{a}_h(\omega)$ and D_{gh}. However, (17) points out that the observations are also characterized by the bearings $\phi_1, \ldots, \phi_H$ to the source from the individual arrays and the relative time delays D_{gh} between pairs of arrays.[2] Therefore, one way to estimate the source location (x_s, y_s) is to first estimate the bearings $\phi_1, \ldots, \phi_H$ and the pairwise time delays D_{gh}. A significant advantage of this approach is that it allows application of the vast amount of knowledge and techniques that are available for bearing estimation with single arrays, as well as time delay estimation with two sensors. Once the bearings $\phi_1, \ldots, \phi_H$ and the time delays D_{gh} are estimated, the source location (x_s, y_s) is estimated by "triangulating" with the equations

$$\cos(\phi_h) = \frac{x_s - x_h}{[(x_s - x_h)^2 + (y_s - y_h)^2]^{1/2}}, \quad h = 1, \ldots, H \tag{18}$$

$$\sin(\phi_h) = \frac{y_s - y_h}{[(x_s - x_h)^2 + (y_s - y_h)^2]^{1/2}}, \quad h = 1, \ldots, H \tag{19}$$

$$D_{gh} = \frac{1}{c}\left[(x_s - x_g)^2 + (y_s - y_g)^2\right]^{1/2} - \frac{1}{c}\left[(x_s - x_h)^2 + (y_s - y_h)^2\right]^{1/2}, \quad \begin{array}{l} h = 2, \ldots, H \\ g = 1, \ldots, h-1 \end{array} \tag{20}$$

Methods for efficiently solving (18) to (20) for (x_s, y_s) need to be investigated. Standard solutions are available for triangulating the bearings alone with (18) and (19), but the nonlinear equations in (20) involving the time delays complicates the problem.

3 CRBs on Localization Accuracy

The problem of interest is to estimate the source location parameter vector $\mathbf{\Theta} = [x_s, y_s]^T$ using T samples of the sensor signals $\mathbf{Z}(0), \mathbf{Z}(T_s), \ldots, \mathbf{Z}((T-1) \cdot T_s)$, where T_s is the sampling period. Let us denote the sampling rate by $f_s = 1/T_s$ and $\omega_s = 2\pi f_s$. We will assume that the continuous-time random processes $\mathbf{Z}(t)$ are band-limited, and that the sampling rate f_s is greater than twice the bandwidth of the processes. Then Friedlander [16] has shown, using a theorem of Whittle [17], that the Fisher information matrix (FIM) $\mathbf{J}$ for the parameters $\mathbf{\Theta}$ based on the samples $\mathbf{Z}(0), \mathbf{Z}(T_s), \ldots, \mathbf{Z}((T-1) \cdot T_s)$ has elements

$$J_{ij} = \frac{T}{2\omega_s} \int_0^{\omega_s} \operatorname{tr}\left\{ \frac{\partial \mathbf{G}_{\mathbf{Z}}(\omega)}{\partial \theta_i} \mathbf{G}_{\mathbf{Z}}(\omega)^{-1} \frac{\partial \mathbf{G}_{\mathbf{Z}}(\omega)}{\partial \theta_j} \mathbf{G}_{\mathbf{Z}}(\omega)^{-1} \right\} d\omega, \qquad i, j = 1, 2, \tag{21}$$

where "tr" denotes the trace of the matrix. The CRB matrix $\mathbf{C} = \mathbf{J}^{-1}$ then has the property that the covariance matrix of any unbiased estimator $\hat{\mathbf{\Theta}}$ satisfies $\operatorname{Cov}(\hat{\mathbf{\Theta}}) - \mathbf{C} \geq \mathbf{0}$, where $\geq \mathbf{0}$ means that $\operatorname{Cov}(\hat{\mathbf{\Theta}}) - \mathbf{C}$ is positive semidefinite [15]. The CRB provides a lower bound on the performance of any unbiased estimator. Equation (21) provides a convenient way to compute the FIM for the distributed sensor array model. It provides a powerful tool for evaluating the impact that various parameters have on source localization accuracy. Parameters of interest include the spectral coherence between distributed arrays, the signal bandwidth and power spectrum, the array placement geometry, and the SNR. The FIM in (21) is not easily evaluated analytically, but it is readily evaluated numerically for cases of interest. Next we specialize the FIM expression (21) for two important cases.

[2] In order to recover the source location (x_s, y_s) from the bearings $\phi_1, \ldots, \phi_H$ and the relative time delays D_{gh}, the array geometry must be such that the set of equations (18) to (20) are uniquely invertible.

3.1 Time delay estimation with partial coherence

If we specialize our general model to the case of $H = 2$ arrays containing $N_1 = N_2 = 1$ sensor each, then we have the classic problem of estimating the relative time delay of a signal at two sensors [18]. Using (17), we characterize the observations at the two sensors by the cross-spectral density matrix

$$\mathbf{G_Z}(\omega) = \left[\begin{array}{cc} G_{s,11}(\omega) + G_w(\omega) & e^{-j\omega D_{12}}\, \gamma_{s,12}(\omega)\, \left(G_{s,11}(\omega) G_{s,22}(\omega)\right)^{1/2} \\ e^{+j\omega D_{12}}\, \gamma_{s,12}(\omega)\, \left(G_{s,11}(\omega) G_{s,22}(\omega)\right)^{1/2} & G_{s,22}(\omega) + G_w(\omega) \end{array} \right], \tag{22}$$

which depends only on the time-delay parameter D_{12}. The observation model (22) is more general than the standard time-delay model [18], since it allows partial spectral coherence of the *signal* at the two sensors through the function $\gamma_{s,12}(\omega)$. The standard treatments of time-delay estimation assume perfect coherence of the signal components, i.e., $\gamma_{s,12}(\omega) = 1$.[3] The FIM for the time-delay D_{12} can then be expressed in the form

$$J(D_{12}) = \frac{T}{2\omega_s} \int_0^{\omega_s} \frac{\omega^2\, \gamma_{s,12}(\omega)^2\, \frac{G_{s,11}(\omega) G_{s,22}(\omega)}{G_w(\omega)^2}}{1 + \frac{G_{s,11}(\omega)}{G_w(\omega)} + \frac{G_{s,22}(\omega)}{G_w(\omega)} + \left[1 - \gamma_{s,12}(\omega)^2\right] \frac{G_{s,11}(\omega) G_{s,22}(\omega)}{G_w(\omega)^2}}\, d\omega. \tag{23}$$

The FIM (23) reduces to the well-known result in the time-delay literature [19, 16, 18] when the signal is perfectly coherent between the sensors $\gamma_{s,12}(\omega) = 1$.

3.2 Narrowband signals with distributed arrays

Next we consider the case with H distributed arrays containing $N_1, \ldots, N_H$ sensors each, but with an acoustic source that has a *narrowband* power spectrum. That is, the PSD $G_{s,hh}(\omega)$ of the signal at each array $h = 1, \ldots, H$ is nonzero only in a narrow band of frequencies $\omega_0 - (\Delta\omega/2) \leq \omega \leq \omega_0 + (\Delta\omega/2)$. If the bandwidth $\Delta\omega$ is chosen small enough so that the $\omega-$dependent quantities in (21) are well approximated by their value at ω_0, then the narrowband approximation to the FIM (21) is

$$J_{ij} \approx \frac{T\Delta\omega}{\omega_s} \mathrm{tr} \left\{ \frac{\partial\, \mathbf{G_Z}(\omega_0)}{\partial\, \theta_i}\, \mathbf{G_Z}(\omega_0)^{-1} \frac{\partial\, \mathbf{G_Z}(\omega_0)}{\partial\, \theta_j}\, \mathbf{G_Z}(\omega_0)^{-1} \right\}. \tag{24}$$

The quantity $\frac{T\Delta\omega}{\omega_s}$ multiplying the FIM in (24) is the time-bandwidth product of the observations. In order for the narrowband approximation to be valid, the fractional bandwidth $\Delta\omega/\omega_0$ must be small. If we consider a typical acoustic signal processing application in which the frequencies of interest ω_0 are in the range from $2\pi(50)$ to $2\pi(250)$ rad/sec, then a reasonable value for $\Delta\omega$ is 2π, representing a 1-Hz bandwidth. We will use $\Delta\omega = 2\pi$ in the examples of narrowband processing presented in Section 4.

[3] We should point out that the literature on time-delay estimation makes extensive use of the so-called "coherence function." However, the coherence function in the time delay literature is *not* $\gamma_{s,12}(\omega)$, which characterizes the signal coherence. Instead, the coherence function in the time-delay literature is related to the noisy observations $z_{11}(t), z_{21}(t)$ defined by (12). Specifically, it is the normalized cross-spectral density of $z_{11}(t)$ and $z_{21}(t)$, i.e.:

$$\gamma_{z,12}(\omega) = \exp(-j\omega D_{12}) \left(1 + \frac{G_w(\omega)}{G_{s,11}(\omega)}\right)^{-1/2} \left(1 + \frac{G_w(\omega)}{G_{s,22}(\omega)}\right)^{-1/2}.$$

Thus any loss in spectral coherence in $\gamma_{z,12}(\omega)$ is due to the additive noise PSD $G_w(\omega)$, and not loss of signal coherence during propagation.

The narrowband FIM (24) extends in a simple way to the case of acoustic sources that contain multiple narrowband frequency components centered at $\omega_1, \ldots, \omega_F$:

$$J_{ij} \approx \frac{T\Delta\omega}{\omega_s} \sum_{k=1}^{F} \operatorname{tr}\left\{ \frac{\partial\, \mathbf{G}_{\mathbf{Z}}(\omega_k)}{\partial\, \theta_i} \mathbf{G}_{\mathbf{Z}}(\omega_k)^{-1} \frac{\partial\, \mathbf{G}_{\mathbf{Z}}(\omega_k)}{\partial\, \theta_j} \mathbf{G}_{\mathbf{Z}}(\omega_k)^{-1} \right\}. \tag{25}$$

3.3 CRB for schemes with reduced communication bandwidth

The CRBs presented so far in this section provide a performance bound on source location estimation methods that jointly process all the data from all the sensors. Such processing provides the best attainable results, but it also requires significant communication bandwidth to transmit data from the individual arrays to the fusion center. In this subsection, we develop approximate performance bounds on schemes that perform bearing estimation at the individual arrays in order to reduce the required communication bandwidth to the fusion center. These CRBs facilitate a study of the tradeoff between source location accuracy and communication bandwidth between the arrays and the fusion center.

First we consider the simplest scheme in which each array transmits only its bearing estimate to the fusion center. The fusion center then triangulates the bearings $\phi_1, \ldots, \phi_H$ to estimate the source location (x_s, y_s) using (18) and (19). This scheme independently processes the data from each array to estimate the bearings, so it does not exploit coherence of the signal at the arrays. Therefore the performance of this scheme must be no better than the performance of the optimum scheme with incoherent signals, i.e., with $\gamma_{s,gh}(\omega) = 0$ for all $g < h$ and all ω. We use the CRB of the optimum scheme with incoherent signals at all arrays to bound the performance of triangulation with bearing estimates.

Next we consider a scheme in which each array transmits its bearing estimate *and* the T samples from one sensor to the fusion center. We assume that the sensor whose samples are transmitted is located at the reference location (x_h, y_h) for the array. In this case the fusion center is able to exploit signal coherence at distributed arrays by estimating the time delays D_{gh}. However, coherence is not exploited in the estimation of the bearings.

We approximate the performance bound for this scheme as follows. To simplify the modeling, we assume the existence of an independent sensor at the reference location (x_h, y_h) of each array. The samples from this independent sensor are transmitted to the fusion center, but they are not used for bearing estimation. Similar to (12), the observations at these additional sensors are modeled as

$$\bar{z}_h(t) = s_h(t - \tau_h) + \bar{w}_h(t), \quad h = 1, \ldots, H, \tag{26}$$

where the noise $\bar{w}_h(t)$ is independent from the noise at all other sensors and shares the common noise PSD $G_w(\omega)$. We define a vector $\bar{\mathbf{z}}(t) = [\bar{z}_1(t), \ldots, \bar{z}_H(t)]^T$ and a larger vector $\bar{\mathbf{Z}}(t) = [\mathbf{Z}(t)^T, \bar{\mathbf{z}}(t)^T]^T$ that collects all of the sensor signals in this model. In order to reflect the fact that the signal coherence is not exploited in the bearing estimation using $\mathbf{Z}(t)$ while it is exploited in the estimation of the time delays D_{gh} using $\bar{z}_h(t)$, the cross-spectral density matrix of $\bar{\mathbf{Z}}(t)$ is modeled as

$$\mathbf{G}_{\bar{\mathbf{Z}}}(\omega) = \begin{bmatrix} \mathbf{G}_{\mathbf{Z}}^{(\mathrm{B})}(\omega) & \mathbf{0} \\ \mathbf{0} & \mathbf{G}_{\bar{\mathbf{z}}}^{(\mathrm{TD})}(\omega) \end{bmatrix}, \tag{27}$$

where $\mathbf{G}_{\mathbf{Z}}^{(\mathrm{B})}(\omega)$ is formed from (17) assuming incoherent signals for bearing estimation

$$\mathbf{G}_{\mathbf{Z}}^{(\mathrm{B})}(\omega) = \begin{bmatrix} \mathbf{a}_1(\omega)\mathbf{a}_1(\omega)^H G_{s,11}(\omega) & \cdots & \mathbf{0} \\ \vdots & \ddots & \vdots \\ \mathbf{0} & \cdots & \mathbf{a}_H(\omega)\mathbf{a}_H(\omega)^H G_{s,HH}(\omega) \end{bmatrix} + G_w(\omega)\mathbf{I}, \tag{28}$$

and $\mathbf{G}_{\bar{\mathbf{z}}}^{(\mathrm{TD})}(\omega)$ includes the signal coherence to allow time-delay (TD) estimation

$$\mathbf{G}_{\bar{\mathbf{z}}}^{(\mathrm{TD})}(\omega) = \begin{bmatrix} G_{s,11}(\omega) + G_w(\omega) & \cdots & e^{-j\omega D_{1H}}\gamma_{s,1H}(\omega)\ (G_{s,11}(\omega)G_{s,HH}(\omega))^{1/2} \\ \vdots & \ddots & \vdots \\ e^{+j\omega D_{1H}}\gamma_{s,1H}(\omega)\ (G_{s,11}(\omega)G_{s,HH}(\omega))^{1/2} & \cdots & G_{s,HH}(\omega) + G_w(\omega) \end{bmatrix}. \tag{29}$$

We obtain the FIM for estimation of the source location parameters (x_s, y_s) using this scheme by inserting $\mathbf{G}_{\bar{\mathbf{Z}}}(\omega)$ in (27) into the general expression (21). The existence of H independent sensors for time-delay estimation is assumed so that (27) becomes block-diagonal to decouple the bearing and time-delay parameters. In practice, the use of the same sensor for bearing estimation and time-delay estimation will have little effect on the estimation performance. Note that the model assumes that the fusion processor estimates the time-delays D_{gh} for $h = 2, \ldots, H, \quad g = 1, \ldots, h$ *jointly* based on the time samples $\bar{\mathbf{z}}(1), \ldots, \bar{\mathbf{z}}(T)$. A practical time-delay estimation method is likely to estimate only the $H-1$ time delays $D_{12}, \ldots, D_{1H}$ through independent, pairwise processing of the sensor samples. Such a pairwise processing scheme cannot perform better than the CRB based on (27). However, results of Weinstein [12] regarding pairwise processing of sensor signals on a single array suggest that the performance degradation is negligible as long as the SNR is greater than 0 dB. It is possible to obtain an exact CRB for pairwise time delay estimation using our model by following Weinstein's approach [12]. However, the exact CRB is considerably more complicated and is valuable only for low SNR scenarios.

4 Examples

In this section, examples are presented that illustrate the improvement in source localization accuracy when coherence between the distributed arrays is exploited. We consider scenarios with $H = 2$ and $H = 3$ arrays. The individual arrays are identical and contain $N_1 = \cdots = N_H = 7$ sensors. Each array is circular and has 4-ft radius, with six sensors equally spaced around the perimeter and one sensor in the center. Narrowband processing in a 1-Hz band centered at 50 Hz is assumed, with an SNR of 10 dB at each sensor, i.e., $G_{s,hh}(\omega)/G_w(\omega) = 10$ for $h = 1, \ldots, H$ and $2\pi(49.5) < \omega < 2\pi(50.5)$ rad/sec. The signal coherence $\gamma_{s,12}(\omega) = \gamma_s(\omega)$ is varied between 0 and 1. We assume that $T = 4000$ time samples are obtained at each sensor with sampling rate $f_s = 2000$ samples/sec. The source localization performance is evaluated by plotting the ellipse in (x, y) coordinates that satisfy the expression

$$\begin{bmatrix} x & y \end{bmatrix} \mathbf{J} \begin{bmatrix} x \\ y \end{bmatrix} = 1, \tag{30}$$

where $\mathbf{J}$ is the FIM. If the errors in (x, y) localization are jointly Gaussian distributed, then the ellipse (30) represents the contour at one standard deviation in root-mean-square (RMS) error. The error ellipse for any unbiased estimator of source location cannot be smaller than the ellipse described by (30).

First we consider a scenario with $H = 2$ arrays located at coordinates $(x_1, y_1) = (0, 0)$, $(x_2, y_2) = (400, 400)$, and one source located at $(x_s, y_s) = (200, 300)$, where the units are meters. The array and source locations are illustrated in Figure 2a, along with the RMS error ellipse for joint processing of all sensor data for coherence values $\gamma_s(\omega) = 0, 0.5$, and 1. The largest ellipse in Figure 2a corresponds to incoherent signals $\gamma_s(\omega) = 0$ and characterizes the performance of the simple method

of triangulation using the bearing estimates from the two arrays. Note that signal coherence between the arrays significantly reduces the width of the ellipse along one axis. However, the localization along the other axis of the ellipse is not reduced by coherence. This is because the two widely separated arrays are able to accurately localize the *bearing* of the source but not its range. Figure 2b shows the ellipse radius for various values of the signal coherence $\gamma_s(\omega)$. Note that even a small amount of coherence produces a significant improvement in localization accuracy. Note also that for this scenario, the localization scheme based on bearing estimation with each array and time-delay estimation using one sensor from each array performs equivalently to the optimum, joint processing scheme. Figure 2c shows a closer view of the error ellipses for the scheme of bearing estimation plus time-delay estimation with one sensor from each array. The ellipses are identical to those in Figure 2a for joint processing.

Figure 3 displays the results when a third array is added at location $(x_3, y_3) = (100, 0)$. The coherence between all pairs of arrays is assumed to be identical, i.e., $\gamma_{s,gh}(\omega) = \gamma_s(\omega)$ for $(g, h) = (1, 2), (1, 3), (2, 3)$. Note that increased signal coherence allows improved source localization along both axes of the ellipse. The largest ellipse in Figure 3a is the incoherent case, characterizing the performance of triangulation with independent bearing estimates. Figure 3b shows that a significant improvement in localization accuracy is possible with the small value of coherence $\gamma_s(\omega) = 0.1$, with continued improvement as the coherence increases. As in Figure 2, the method of bearing estimation plus time delay estimation using one sensor from each array performs nearly as well as joint processing.

These results indicate that even small amounts of signal coherence between widely distributed arrays provides the potential for significant improvement in source localization accuracy. We point out that the CRB results for time-delay estimation in this case are optimistic due to the narrowband model for the observations. With narrowband signals at 50 Hz, the time delays are resolvable only within the interval of one period of $(50\,\mathrm{Hz})^{-1} = 0.02$ sec. The CRB assumes that the ambiguities on the order of 0.02 seconds are resolved by an unbiased estimator. Modeling the signal as wideband removes this ambiguity in time-delay estimation.

5 Concluding Remarks

We have presented a model in this paper for source localization with distributed sensor arrays. The model is general and may be used to represent sources with arbitrary power spectrum and frequency-dependent coherence between the distributed arrays. The model assumes perfect wavefront coherence across individual arrays in order to focus attention on the value of coherence at distributed arrays.

The following are some items of current and future work based on this model.

- Combine the general model and performance analysis in this paper with physical models for the coherence and source power spectrum as in Wilson [10, 13, 14].
- Analyze the sensitivity of various schemes for processing signals from distributed arrays to uncertainty in time synchronization and position of the arrays.
- Study the performance versus complexity tradeoff for schemes that further reduce the communication bandwidth between the distributed arrays and the central fusion center. For example, study methods for compressing the sampled data from distributed sensors so that the cross-correlation properties are preserved for time-delay estimation.

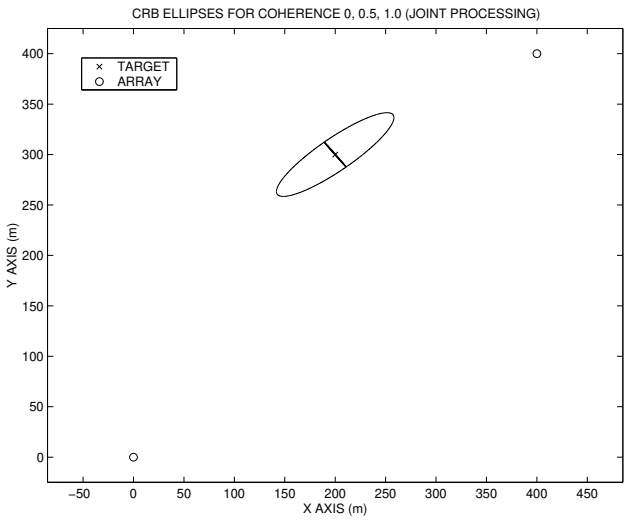

(a)

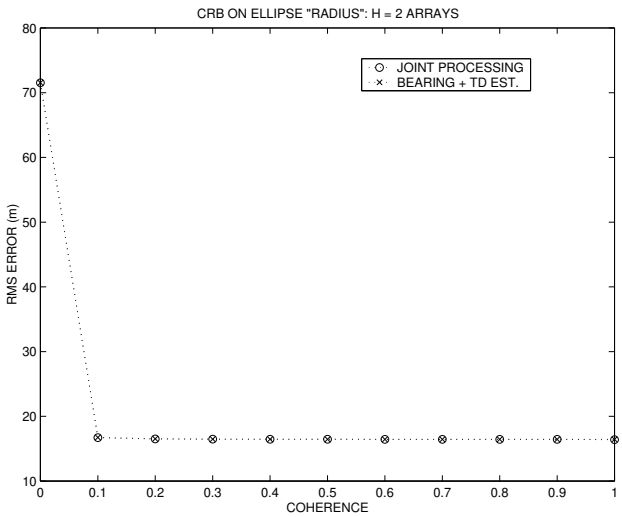

(b)

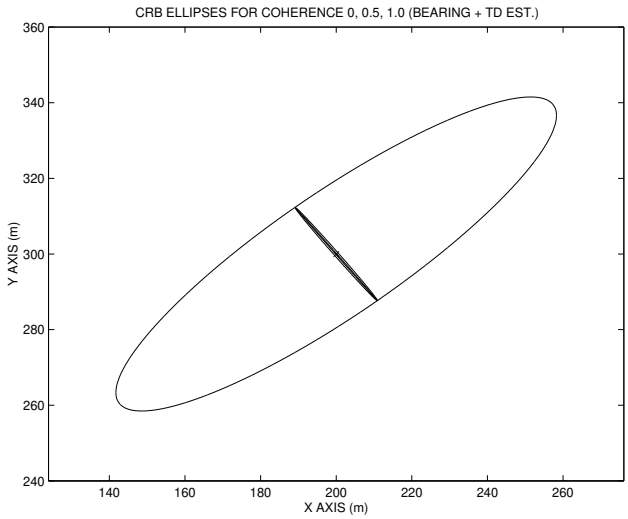

(c)

Figure 2: RMS source localization error ellipses based on the CRB for $H = 2$ arrays and one source. The array and source locations are shown in (a), along with the error ellipses for joint processing of all sensor data for coherence values $\gamma_s(\omega) = 0, 0.5$, and 1. Part (b) shows the error ellipse radius $\left[(\text{major axis})^2 + (\text{minor axis})^2\right]^{1/2}$ for a range of coherence values, comparing joint processing with the reduced-complexity scheme of bearing estimation plus time-delay estimation using data from one sensor per array. Part (c) is a closer view of the RMS error ellipses for the bearing plus time-delay estimation scheme.

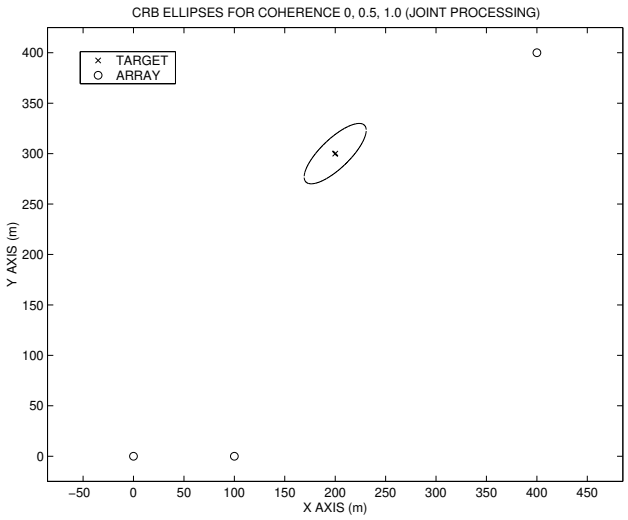

(a)

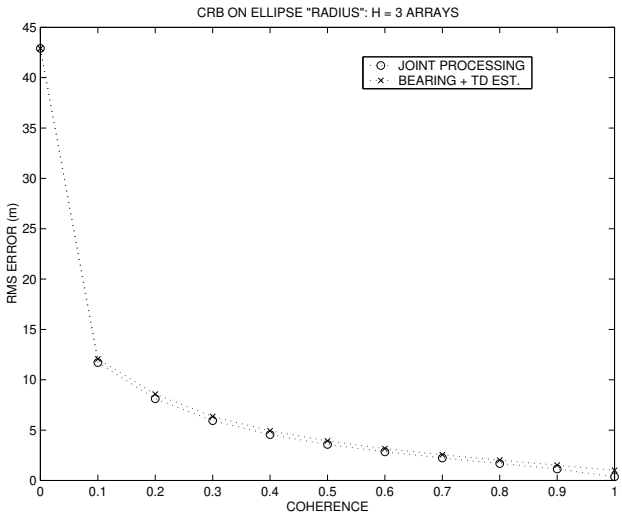

(b)

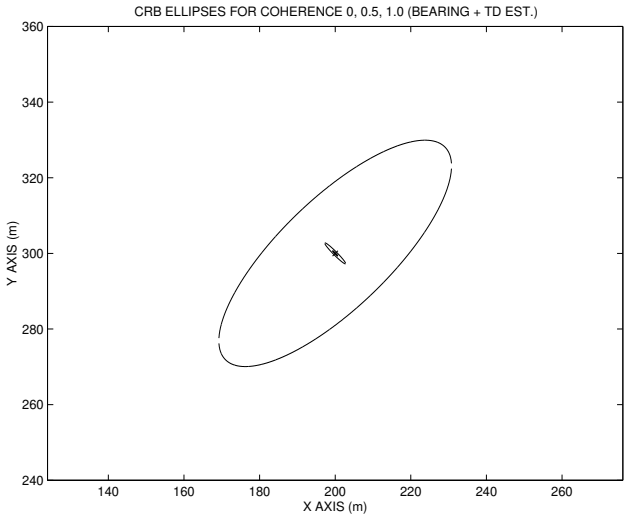

(c)

Figure 3: RMS source localization error ellipses based on the CRB for $H = 3$ arrays and one source.

- The source is assumed to be stationary (not moving) in this paper. A natural way to incorporate source movement into our model is to parameterize the source motion and then estimate the motion parameters instead of the static location (x_s, y_s). However, a joint localization/tracking algorithm of this sort may require different schemes for distributed processing.
- Extend the model and the processing to include multiple sources.

Appendix

A Glossary of Symbols

$E\{\cdot\}$**:** Expectation operation

Superscript $T, *, H$**:** Transpose, complex conjugate, and conjugate transpose, respectively.

(x_s, y_s)**:** Location of source

H**:** Number of arrays

N_h**:** Number of sensors in array h

(x_h, y_h)**:** Location of reference sensor on array h

r_h**:** Distance from source to reference sensor on array h.

$(\Delta x_{hn}, \Delta y_{hn})$**:** Location of sensor n on array h, relative to (x_h, y_h)

c**:** Wave propagation speed

τ_h**:** Propagation time from source to reference sensor on array h

τ_{hn}**:** Propagation time from source to sensor n on array h

$s_h(t - \tau_h - \tau_{hn})$**:** Time signal received at sensor n on array h due to the source (no noise)

$\mathbf{s}(t) = [s_1(t), \ldots, s_H(t)]^T$**:** Vector of source signals received at arrays

$r_{s,gh}(\tau) = E\{s_g(t+\tau)\, s_h(t)\}$**:** Cross-correlation function between signals received at arrays g, h

$\mathbf{R}_s(\tau) = E\{\mathbf{s}(t+\tau)\, \mathbf{s}(t)^T\}$**:** Cross-correlation function matrix

$\mathcal{F}\{\cdot\}$ and $\mathcal{F}\{\cdot\}^{-1}$**:** Fourier transform and inverse Fourier transform operations

$G_{s,gh}(\omega) = \mathcal{F}\{r_{s,gh}(\tau)\}$**:** Cross-spectral density function of signals at arrays g and h

$G_{s,hh}(\omega)$**:** Power spectral density (PSD) of signal at array h

$\mathbf{G}_s(\omega) = \mathcal{F}\{\mathbf{R}_s(\tau)\}$**:** Cross-spectral density matrix

$\gamma_{s,gh}(\omega) = \dfrac{G_{s,gh}(\omega)}{[G_{s,gg}(\omega) G_{s,hh}(\omega)]^{1/2}}$**:** Spectral coherence function of source signals

$p_{s,gh}(\tau) = \mathcal{F}^{-1}\{\gamma_{s,gh}(\omega)\}$**:** Inverse Fourier transform of coherence function

$w_{hn}(t)$**:** Additive noise at sensor n on array h

$r_w(\tau)$ and $G_w(\omega)$**:** Noise autocorrelation function and power spectral density

$z_{hn}(t)$**:** Observed signal at sensor n on array h (due to source and noise)

$\mathbf{z}_h(t) = [z_{h1}(t), \ldots, z_{h,N_h}(t)]^T$**:** Vector of observations at array h

$\mathbf{Z}(t) = [\mathbf{z}_1(t)^T, \ldots, \mathbf{z}_H(t)^T]^T$**:** Vector of observations from all arrays

$\mathbf{a}_h(\omega)$**:** Array manifold for array h at frequency ω

ϕ_h**:** Bearing of source with respect to array h

$D_{gh} = \tau_g - \tau_h$**:** Relative time delay of the signal at arrays g and h

$\mathbf{G}_{\mathbf{Z}}(\omega)$**:** Cross-spectral density matrix of $\mathbf{Z}(t)$

$\mathbf{J}$**:** Fisher information matrix (FIM)

T**:** Number of time samples observed at sensors

f_s, ω_s**:** Sampling rate in hertz and rad/sec, respectively

$T_s = 1/f_s$**:** Spacing between time samples

$\bar{z}_h(t)$**:** Observed signal at independent sensors used for time-delay estimation, and vectors:
$\bar{\mathbf{z}}(t) = [\bar{z}_1(t), \ldots, \bar{z}_H(t)]^T, \qquad \bar{\mathbf{Z}}(t) = [\mathbf{Z}(t)^T, \bar{\mathbf{z}}(t)^T]^T$

$\mathbf{G}_{\bar{\mathbf{Z}}}(\omega)$**:** Cross-spectral density matrix of $\bar{\mathbf{Z}}(t)$

$\mathbf{G}_{\mathbf{Z}}^{(\mathrm{B})}(\omega), \mathbf{G}_{\bar{\mathbf{z}}}^{(\mathrm{TD})}(\omega)$**:** Cross-spectral density matrices for independent bearing and time-delay estimation

References

[1] T. Pham and B. M. Sadler, "Aeroacoustic wideband array processing for detection and tracking of ground vehicles," *130th Meeting of the Acoustic Society of America,* St. Louis, MI, *JASA* vol. 98, no. 5, pt. 2, p. 2969, 1995.

[2] T. Pham and B. M. Sadler, "Adaptive wideband aeroacoustic array processing," *8th IEEE Statistical Signal and Array Processing Workshop,* pp. 295–298, Corfu, Greece, June 1996.

[3] T. Pham and B. Sadler, "Incoherent and coherent wideband direction finding algorithms for ground vehicles," *132nd Meeting of the Acoustic Society of America, JASA* vol. 100, no. 4, pt. 2, p. 2636, October 1996.

[4] T. Pham and B. M. Sadler, "Focused wideband array processing algorithms for high-resolution direction finding," *IRIS Battlefield Acoustics Symposium,* October 1998.

[5] H. Wang and M. Kaveh, "Coherent signal-subspace processing for the detection and estimation of angles of arrival of multiple wide-band sources," *IEEE Trans. Acoust., Speech, Signal Processing*, vol. ASSP-33, pp. 823-831, August 1985.

[6] B. M. Sadler, "Focused wideband maximum likelihood and spatial spectrum estimation" *920th Meeting of the American Mathematical Society,* invited presentation for Special Session on Harmonic Analysis and Applications, College Park, MD, April 1997.

[7] A. Paulraj and T. Kailath, "Direction of arrival estimation by eigenstructure methods with imperfect spatial coherence of wavefronts," *J. Acoust. Soc. Am.*, vol. 83, pp. 1034-1040, March 1988.

[8] A.B. Gershman, C.F. Mecklenbrauker, J.F. Bohme, "Matrix fitting approach to direction of arrival estimation with imperfect spatial coherence," *IEEE Trans. on Signal Proc.*, vol. 45, no. 7, pp. 1894-1899, July 1997.

[9] B.-G. Song and J.A. Ritcey, "Angle of arrival estimation of plane waves propagating in random media," *J. Acoust. Soc. Am.*, vol. 99, no. 3, pp. 1370-1379, March 1996.

[10] D.K. Wilson, "Performance bounds for acoustic direction-of-arrival arrays operating in atmospheric turbulence," *J. Acoust. Soc. Am.*, vol. 103, no. 3, pp. 1306-1319, March 1998.

[11] M. Wax and T. Kailath, "Decentralized processing in sensor arrays," *IEEE Trans. on Acoustics, Speech, Signal Processing*, vol. ASSP-33, no. 4, pp. 1123-1129, October 1985.

[12] E. Weinstein, "Decentralization of the Gaussian maximum likelihood estimator and its applications to passive array processing," *IEEE Trans. Acoust., Speech, Sig. Proc.*, vol. ASSP-29, no. 5, pp. 945-951, October 1981.

[13] D.K. Wilson, "Atmospheric effects on acoustic arrays: a broad perspective from models," *1999 Meeting of the IRIS Specialty Group on Battlefield Acoustics and Seismics*, Laurel, MD, September 13-15, 1999.

[14] D.K. Wilson, G.L. Szeto, B.M. Sadler, R. Adams, N. Srour, "Propagation and array performance modeling for acoustic tracking of cruise missiles," *1999 Meeting of the IRIS Specialty Group on Battlefield Acoustics and Seismics*, Laurel, MD, September 13-15, 1999.

[15] S.M. Kay, *Fundamentals of Statistical Signal Processing: Estimation Theory*, Prentice-Hall, 1993.

[16] B. Friedlander, "On the Cramer-Rao Bound for Time Delay and Doppler Estimation," *IEEE Trans. on Info. Theory*, vol. IT-30, no. 3, pp. 575-580, May 1984.

[17] P. Whittle, "The analysis of multiple stationary time series," *J. Royal Statist. Soc.*, vol. 15, pp. 125-139, 1953.

[18] G.C. Carter (ed.), *Coherence and Time Delay Estimation* (Selected Reprint Volume), IEEE Press, 1993.

[19] C.H. Knapp and G.C. Carter, "The generalized correlation method for estimation of time delay," *IEEE Trans. on Acoustics, Speech, Signal Processing*, vol. ASSP-24, no. 4, pp. 320-327, August 1976.